Title

Recovery of Rare Earth Elements from Geothermal Fluids through Bacterial Cell Surface Adsorption

Journal

Environmental Science and Technology, 53(13)

ISSN

0013-936X

Authors

Brewer, Aaron
Chang, Elliot
Park, Dan M
et al.

Publication Date

2019-07-02

DOI

10.1021/acs.est.9b00301

Peer reviewed

Environmental Science & Technology

Article

Cite This: Environ. Sci. Technol. XXXX, XXX, XXX−XXX

pubs.acs.org/est

Recovery of Rare Earth Elements from Geothermal Fluids through Bacterial Cell Surface Adsorption

Aaron Brewer,[†,‡] Elliot Chang,[§] Dan M. Park,[†] Tianyi Kou,[∥] Yat Li,[∥] Laura N. Lammers,[§] and Yongqin Jiao*[,†]

[†]Physical and Life Science Directorate, Lawrence Livermore National Laboratory, Livermore, California 94550, United States

[‡]Department of Earth and Space Sciences, University of Washington, Seattle, Washington 98185, United States

[§]Department of Environmental Science, Policy, and Management, University of California Berkeley, Berkeley, California 94270, United States

[∥]Chemistry and Biochemistry Department, University of California Santa Cruz, Santa Cruz, California 95064, United States

Supporting Information

ABSTRACT: The increasing demand for rare earth elements (REEs) in the modern economy motivates the development of novel strategies for cost-effective REE recovery from non-traditional feedstocks. We previously engineered *E. coli* to express lanthanide binding tags on the cell surface, which increased the REE biosorption capacity and selectivity. Here we examined how REE adsorption by the engineered *E. coli* is affected by various geochemical factors relevant to geothermal fluids, including total dissolved solids (TDS), temperature, pH, and the presence of specific competing metals. REE biosorption is robust to TDS, with high REE recovery efficiency and selectivity observed with TDS as high as 165,000 ppm. Among several metals tested, U, Al, and Pb were found to be the most competitive, causing >25% reduction in REE biosorption when present at concentrations ∼3- to 11-fold higher than the REEs. Optimal REE biosorption occurred between pH 5−6, and sorption capacity was reduced by ∼65% at pH 2. REE recovery efficiency and selectivity increased as a function of temperature up to ∼70 °C due to the thermodynamic properties of metal complexation on the bacterial surface. Together, these data define the optimal and boundary conditions for biosorption and demonstrate its potential utility for selective REE recovery from geofluids.

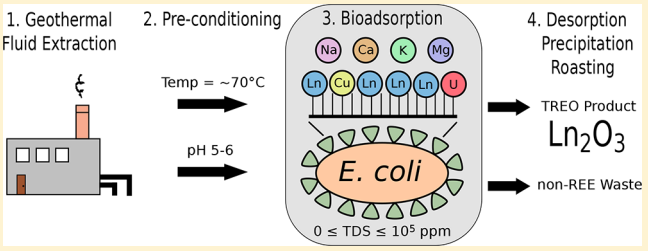

INTRODUCTION

Rare earth elements (REEs) are becoming increasingly significant to the international economy with the emergence and development of new technologies, particularly in the area of clean energy. Common applications of REEs include automotive and industrial catalysts, permanent magnets, and electronics.[1−3] However, the supply of these metals is uncertain and potentially at risk globally. As of 2011, more than 95% of REE production came from China, even though there are significant reserves worldwide.[1] Given the limited sources of REE production and the increasing demand for these metals around the world, it is crucial to explore new REE feedstocks and to develop new and improved methods of REE extraction.[1,4−7]

Biosorption has gained interest in recent years as a potential clean, sustainable method to concentrate and purify REEs. The high binding affinity of native cell surfaces for REEs relative to most non-REEs permits the selective adsorption of these valuable metals from low-grade feedstocks.[6,8−10] Microbes are relatively inexpensive to produce in large quantities, and native biomass has a naturally high capacity and selectivity for REE adsorption.[6,11−15] Cell surfaces can withstand multiple cycles of adsorption and desorption, enabling reuse of biomass.[16] Furthermore, biosorption processes are not expected to contribute hazardous chemical wastes to a REE extraction scheme, unlike some conventional methods such as solvent extraction.[17,18] Microbial surface adsorption could present a clean and effective means to concentrate and purify REEs from a variety of feedstocks, including those that are low-grade and traditionally unexploited.

We have previously bioengineered *Escherichia coli* to express lanthanide binding tags (LBTs) on the cell surface to enhance their natural adsorptive properties, improving both extraction efficiency and selectivity for REEs.[19] While the native cell surface functional groups, primarily carboxylates,[20−23] contribute significantly to REE adsorption, the high-density LBT display increased the relative affinity of the cell surface for REEs over all non-REEs except for Cu.[17] This high REE selectivity is especially critical with low-grade feedstocks where REE content is extremely low compared to many non-REE metals. In this study, we investigate the REE adsorption performance of the engineered LBT-displayed strain of *E. coli*

Received: January 16, 2019
Accepted: May 30, 2019

DOI: 10.1021/acs.est.9b00301
Environ. Sci. Technol. XXXX, XXX, XXX−XXX

Table 1. Chemical Composition of Several Geofluids[a]

	total REEs (ppb)	Na (ppm)	Mg (ppm)	K (ppm)	Ca (ppm)	Fe (ppm)	Cu (ppb)	Pb (ppb)	U (ppb)	Th (ppt)	Al (ppb)	pH
Sangan Thermal Spring, Iran[60]	3170	882	152	477	752	61000	n/a	n/a	n/a	n/a	2420	1.2
Obuki Hot Spring, Japan[61]	220	34	32.8	31	104	52.2	n/a	n/a	n/a	n/a	95	1.35
Dagunguo Spring, China[62]	87.7	1820	0.07	745	1.26	0.0394	1.16	3.13	0.19	0.21	0.17	8.27
Valles Caldera, USA[63]	339	12.2	n/a	81	115	92.4	n/a	n/a	n/a	n/a	170	1.33
Salton Sea, USA[63]	1.32	60500	n/a	18800	31100	1580	n/a	n/a	n/a	n/a	bd	5.70
Blue Mountain Geofluid, USA	bd	1370	2.06	150	21.6	0.737	0.25	bd	bd	bd	105	6.15
Y34 Horseshoe Spring[32]	98.0	165	0.500	61.4	4.81	2.07	n/a	n/a	n/a	n/a	2480	3.5
Great Salt Lake, U.S.A.	0.390	25700	2590	2050	162	n/a	n/a	n/a	5.84	6.60	164	7.92

[a]Data not available is reported as "n/a", and below detection limit is reported as "bd".

under various geochemical conditions characteristic of geofluids.

Geothermal fluids are abundant, low-grade feedstocks that are currently being investigated as a potential source of REEs.[6,8,24,25] Total REE concentrations reported in geofluids range from subppb to low-ppm levels.[26] Fluids with REE concentrations at ppb levels or higher are nearly always acidic (pH < 3.5), likely due to increased metal leaching at lower pH.[24,26] Optimal REE biosorption typically occurs at pH ≈ 6 and decreases with pH; therefore, pH adjustment may be required for the acidic, REE-rich feedstocks.[16,27,28] The temperature of geofluids varies greatly, and previous studies have demonstrated that temperatures as high as 80 °C can lead to increased REE adsorption onto organic surfaces.[28−30] Total dissolved solids (TDS) in geofluids can be as high as hundreds of thousands of ppm, several orders of magnitude higher than the REEs.[26] The major contributors to TDS, such as Na and Mg, have low affinities for cell surface binding sites compared to the REEs but are present at such high concentrations that they may still be competitive. In addition, some metals, such as U and Pb, although present at much lower concentrations, are likely competitive because they have high affinities for the relevant cell surface sites.[19]

Although they have relatively low REE concentrations, geofluids are abundant and have the advantage of requiring minimal pretreatment prior to REE extraction, unlike solid feedstocks such as ores and ion adsorption clays, for which chemical leaching is generally required.[19,25,31] Herein, we systematically examined the effects of TDS, competing metals, pH, and temperature on REE adsorption efficiency and selectivity. Results define the geochemical conditions that are amenable to REE biosorption, information that is key to the future development of a high-performance biosorption technology for REE recovery from geofluids.

METHODS

Bacterial Strains and Growth Conditions. The *E. coli* strain harboring a *lpp-ompA*-dLBT expression plasmid was grown in LB media supplemented with 50 μg/mL ampicillin. Expression of lpp-ompA-dLBT was induced at midexponential phase using 0.002% arabinose for 3 h at 37 °C. For a full description of plasmid construction and LBT expression see Park et al. (2016) and (2017).[16,19] Cells were harvested, washed once in 10 mM MES (2-(*N*-morpholino)-ethanesulfonic acid) pH 6, normalized by OD_{600}, and used in biosorption experiments.

Blue Mountain Geofluid REE Biosorption. A natural geofluid (pH ≈ 6) from the Blue Mountain geothermal area (BMG; NV, U.S.A.; Table 1) was obtained from AltaRock Energy Inc. (WA, U.S.A.). Since the REE concentrations in BMG are <10 ppt, Tb was spiked in at 10 ppb. Cell density was set at ∼1 × 10^8 cells/mL. After 30 min incubation with the BMG, cells were separated by centrifugation at 20 000*g* for 5 min. Cells were washed once in 10 mM MES (pH 6) and resuspended in an equal volume of 5 mM citrate (pH 6) for 60 min for metal desorption. The supernatant was collected for analysis following centrifugation at 20 000*g* for 8 min.

REE Biosorption with the Great Salt Lake Brine. To test the effects of TDS and pH on REE biosorption, we used a synthetic geofluid that resembles the cation composition of the Great Salt Lake brine (GSL) (Table 1). The solution was made from a mixture of chloride and sulfate salts. For the TDS experiment, aliquots of this GSL solution were diluted 3-, 10-, 100-, and 1000-fold using 10 mM MES buffer (pH 6). Tb concentration was set at 100 ppb and cell density at ∼1 × 10^8 cells/mL. Cells were incubated in the spiked brine solutions for 30 min prior to separation via centrifugation at 20 000*g* for 15 min. Then, the cells were washed in 10 mM MES (pH 6) and resuspended in an equal volume of 5 mM citrate pH 6 for 60 min for desorption. The supernatant was collected following centrifugation at 20 000*g* for 5 min. Control experiments with no cells revealed <2% Tb extraction at all TDS conditions.

For the pH experiment, the synthetic GSL solution, diluted 2-fold, was spiked to a final Tb concentration of ∼16 ppm and adjusted to an initial pH of 2−6 using 10 M NaOH. The cells (∼1 × 10^9 cells/mL) were pelleted at 6000*g* for 5 min and resuspended in the respective pH-adjusted GSL feedstock. Following a 30 min incubation, aliquots of the cell suspension were transferred to cellulose acetate centrifuge tube filters (Costar) and spun at 6000*g* for 5 min to collect the cells. The cells on the filters were then washed in 10 mM MES (pH 6) and exposed to an equal volume of 5 mM citrate for 60 min for desorption. The cellulose acetate filters extracted <4% Tb at all tested conditions.

Temperature Dependence. The GSL solution was diluted 2-fold and adjusted to pH 6 using 10 mM MES buffer (pH 6). Tb was added to ∼48 ppm and cell density was set at ∼1 × 10^9 cells/mL. The cells were incubated in the brine for 25 min at 24 °C, 40 °C, or 70 °C. Cells were collected, washed, and the metals were desorbed with 5 mM citrate (pH 6) at room temperature using the centrifuge tube filters as described above. Two additional experiments were conducted in the low-TDS 10 mM MES buffer (pH 6). First, cells (∼1 × 10^9 cells/mL) were exposed to UV radiation or heated to 70 °C and cooled back to room temperature before being exposed to ∼48 ppm Tb. Second, cells (∼1 × 10^9 cells/mL) were exposed to solutions containing ∼48 ppm of an individual metal (Tb, Cu, Mg, K, or Ca) at a range of temperatures from 24 to 70 °C.

DOI: 10.1021/acs.est.9b00301
Environ. Sci. Technol. XXXX, XXX, XXX−XXX

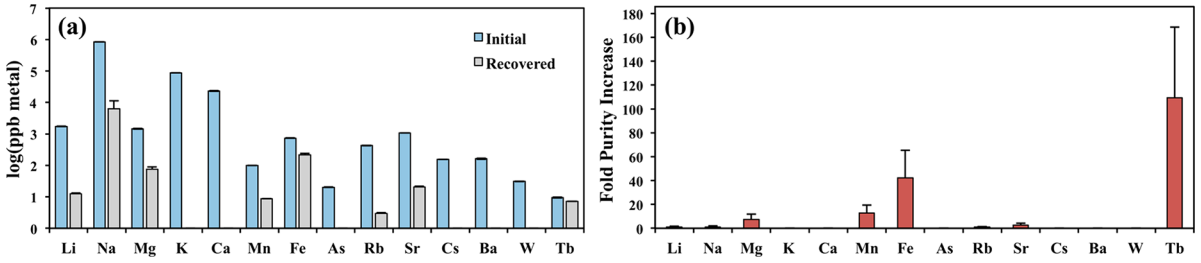

Figure 1. (a) Metal concentrations of the initial REE-spiked Blue Mountain geofluid (blue) and the recovered eluent after biosorption (gray). The initial Tb concentration was 10 ppb and cell concentration was ~1.2×10^8 cells/mL. (b) Fold purity increase for each metal, which is defined for metal x relative to total metals as $(x_{eluent}/total_{eluent})/(x_{feedstock}/total_{feedstock})$. The initial Tb concentration was 10 ppb and cell concentration was at ~1.2×10^8 cells/mL. The error bars represent the standard deviations of biological triplicates.

Metal Competition Experiments. Metal competition experiments were conducted in 10 mM MES buffer (pH 6) by mixing a fixed concentration of Tb (50 μM) with different concentrations of the competing metals, including up to 5000 μM copper (Cu), 300 μM aluminum (Al), 500 μM lead (Pb), 1000 μM uranium (U), 100 μM thorium (Th), 250 mM magnesium (Mg), or 2000 mM sodium (Na). The range of metal concentrations was selected based on concentrations commonly found in geofluids (Table 1).[26] Cell density was set at ~1×10^9 cells/mL, and the adsorption assay was conducted using the centrifugation method as described above.

Horseshoe Spring geofluid REE Biosorption. A synthetic geofluid was made based on the Horseshoe Spring solution from Yellowstone National Park (HS; WY, U.S.A.; Table 1).[32] For the adsorption test, cell density was varied from 0 to 2×10^9 cells/mL. The HS solution was adjusted to pH 3, 4, and 5 prior to exposure to the cells. After 30 min incubation with the HS, cells were separated by centrifugation at 20 000g for 5 min. The supernatant was collected for analysis and the metals adsorbed were calculated via mass balance.

ICP-MS Analysis. Great Salt Lake sample analyses were performed using a Thermo XSeriesII ICP-MS run in standard mode at UC Santa Cruz. The sample introduction system was an ESI PFA-ST nebulizer pumped at 120 μL/min. Blue Mountain Geofluid and Echinus Geyser sample analyses were conducted at Duke University on an Agilent 7900 ICP-MS run in either hydrogen (Ca) or helium gas modes.

Thermodynamic Analysis. The cell surface complexation thermodynamics of REEs can be described by a linear free energy relationship (LFER) that relates aqueous metal-acetate stability constants to calculated metal-bacterial stability constants.[33] Temperature dependent metal-bacteria stability constants are not available for the majority of metals, so we use available data for Zn(II), Cd(II), and Pb(II) complexation with acetate[34] and *Penicillium simplicissimum*[35] at 20, 30, and 40 °C to calibrate T-dependent LFERs (Figure S1 of the Supporting Information, SI). These LFERs maintain high linear correlation coefficients (0.992−0.999) within this temperature range (Figure S1). La-acetate,[36] Na-acetate,[37] Cu-acetate,[34] and UO_2-acetate[38] stability constants were input into each LFER to obtain approximate values for the corresponding metal-bacteria stability constants (Figure S1). We restrict our analysis to between 20 and 40 °C because metal-bacterial stability constants are not yet available for higher temperatures.

Heats of reaction were evaluated using Van't Hoff plots, which relate thermodynamic stability constants to reaction free energies based on the relationship,

$$\ln K = \frac{-\Delta G}{RT} = \frac{\Delta S}{R} - \frac{\Delta H}{R}\left(\frac{1}{T}\right) \quad (1)$$

where ΔG is the Gibbs free energy of reaction, ΔS is the change in entropy, ΔH is the change in enthalpy, R is the gas constant, and T is temperature in °K.

RESULTS AND DISCUSSION

REE Recovery from the Blue Mountain Geothermal Fluid. The low REE concentrations present in most geofluids are a major potential obstacle to economic recovery of REEs from these feedstocks. A natural solution (BMG, pH ≈ 6) from the Blue Mountain geothermal area in Nevada, U.S.A. (Table 1) was selected to test the performance of REE biosorption from geofluids with low REE contents. Because the natural REE concentrations in the BMG are <10 ppt, we spiked the solution with a low concentration (10 ppb) of Tb, a REE of high criticality. Given the low REE concentration, a relatively low cell density (~1×10^8 cells/mL) was used. The results reported here and throughout this study describe the metals recovered during a single adsorption/desorption cycle. Since 5 mM citrate is known to enable complete elution of adsorbed REEs,[16] the extraction efficiencies are controlled by adsorption rather than desorption behavior. At these conditions, LBT-displayed *E. coli* cells[39] extracted ~76% of the available Tb from the spiked BMG (Figure 1a), and extracted <1% of the Na, Li, and Rb and none of the K, Ca, As, Cs, Ba, or W, whose concentrations in the eluent were below the instrumental detection limits (Figure 1a, Table S1). Among the non-REEs, the biosorption process resulted in >1% extraction for only a few elements, Fe (~29%), Mg (~5%), Mn (~9%), and Sr (~2%) (Figure 1, Table S1). These data demonstrate effective and selective adsorption of low concentrations of REEs from a complex geofluid matrix.

Effects of high TDS on REE recovery. The high ratio of total dissolved solids (TDS) to REEs, which in some cases can be on the order of 100,000:1, is a major potential challenge facing efficient recovery of REEs from geofluids.[26] To test the effects of TDS on REE adsorption, we performed REE recovery experiments with a synthetic Great Salt Lake brine (GSL, ~165 000 ppm TDS) that was used either at full strength or diluted 3-, 10-, 100-, and 1000-fold, covering a wide TDS range relevant to geofluids (Table 1). Terbium was added to a final concentration of 100 ppb, which falls on the high end of REE concentrations in natural geofluids (Table 1).[26] Cell density was maintained at ~1.2×10^8 cells/mL to ensure an excess of surface sites for REE adsorption.

REE recovery by the LBT-displayed cells was largely unaffected by TDS under these experimental conditions. At

DOI: 10.1021/acs.est.9b00301
Environ. Sci. Technol. XXXX, XXX, XXX−XXX

low TDS conditions (~5.4 ppm), the LBT-displayed cells extracted ~81.5 ± 4.8% of the available Tb (Figure 2). A slight

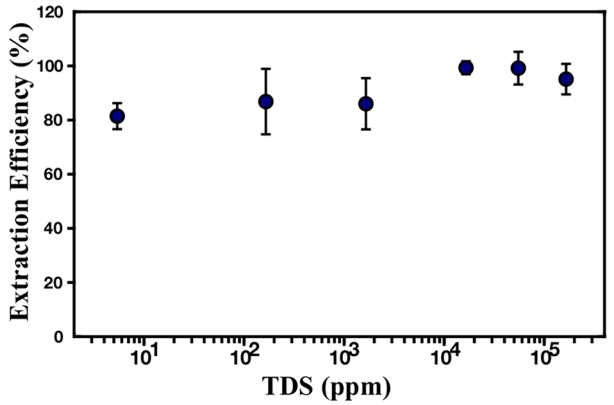

Figure 2. (a) REE adsorption efficiency by LBT-displayed *E. coli* at different total dissolved solid (TDS) concentrations. GSL solution was used at full strength (~165 000 ppm) or diluted 3-, 10-, 100-, 1000-fold. The low salt solution (10 mM MES buffer pH 6, ~5.4 ppm) was included for comparison. The initial Tb concentration was 100 ppb and cell concentration was ~1.2×10^8 cells/mL. The error bars represent the standard deviations of biological triplicates.

increase in Tb recovery was observed at elevated TDS, with ~95.1 ± 5.6% Tb extracted in the concentrated GSL brine (~165 000 ppm; Figure 2). Sodium, potassium, and calcium were not extracted from the initial feedstock, although some Na was contributed by the sodium citrate eluent (Table S2). A small amount of Mg (<2.2 ppm) was extracted across the tested TDS range and did not vary systematically with TDS (Table S2). The observed strong cell surface preference for REEs over the major non-REEs in the GSL brine is consistent with previous studies with other feedstock types, demonstrating the efficacy of biosorption for REE recovery at high TDS conditions.[12,14,40]

Previous reports have found that high TDS can have variable effects on metal adsorption onto a variety of surfaces. Increasing TDS has been shown to decrease REE adsorption onto mineral surfaces, likely due to competition effects from low affinity cations present at high concentrations.[41,42] High TDS is also expected to increase surface charge, weakening the electrostatic attraction between the surface and aqueous metals and decreasing adsorption.[43−45] However, other studies have observed that changes in ionic strength do not affect REE adsorption onto surfaces including chelating polysaccharides,[46] clays,[47] and mesoporous silica.[48] It has been suggested that this REE adsorption is dominated by inner sphere complexation at high affinity sites rather than outer sphere complexation; therefore, the REEs cannot be easily displaced by low affinity ions that constitute the majority of the TDS.[48] On the basis of our findings, at circumneutral pH, the TDS levels typical of geofluids do not strongly affect REE adsorption by LBT-displayed *E. coli*.

Effects of Competing Metals. In addition to high TDS, which is primarily contributed by a few major elements present at high concentrations, REE adsorption efficiency may also be affected by the presence of low concentration metals with a high affinity for the cell surface. Previous experiments with mine tailing leachates identified certain metals, such as Cu, Al, and Pb, that are adsorbed onto the LBT-displayed cell surface alongside the REEs.[19] In addition, uranium and thorium are cogenetic elements during rare earth mineralization and are thus commonly found in REE-bearing minerals.[49,50] These five metals (Cu, Al, Pb, U, and Th) were selected for analysis in a series of competition experiments. Sodium (Na) and magnesium (Mg) were also included for comparison, given their abundance in geofluids, and because Na is often used as a proxy for ionic strength.

In these two-element competition experiments, a fixed concentration of Tb (50 μM, ~8 ppm) was mixed with varying molar concentrations of an individual competing metal and the amount of Tb adsorbed was compared to conditions without the competing metal. The data for each competition experiment was fit by a three-parameter log−logistic function to approximate the competing metal to Tb molar concentration ratio (x/Tb_{25}) at which Tb adsorption is decreased by 25% (Figure 3). We found that U and Al were the most competitive, with x/Tb_{25} values of 3.85 and 4.81, respectively. Lead and copper were less competitive, with x/Tb_{25} values of 10.83 and 63.72, respectively. In contrast, Na (x/Tb_{25} =

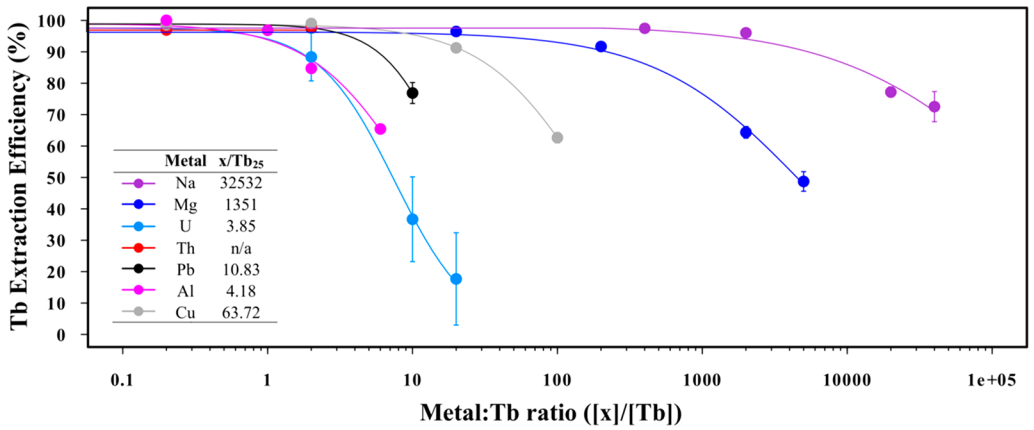

Figure 3. Fraction of terbium (Tb) adsorbed in the presence of a competing metal in buffer solution (10 mM MES pH 6). Initial Tb concentration was fixed at ~8 ppm and cell concentration was fixed at ~1.2×10^9 cells/mL. The data for each competing metal was fit by a three-parameter log−logistic function using the drc (dose response curve) package in R. [x]/[Tb] represents the ratio of the concentration of the competing metal to that of Tb and x/Tb_{25} refers to the value at which Tb adsorption decreases by 25% from that observed in the absence of any competing metal. The error bars represent the standard deviations of biological triplicates.

DOI: 10.1021/acs.est.9b00301
Environ. Sci. Technol. XXXX, XXX, XXX−XXX

32,532) and Mg (x/Tb_{25} = 1351) were much less competitive. The Na competition effect further demonstrates that ionic strength alone has minimal impact on REE adsorption compared to the presence of competitive metals. Terbium adsorption was not affected by Th at the tested concentrations, which cover the range found in most geofluids (Table 1).

The mechanism by which competitive metals displace REEs during adsorption is likely distinct from that of major electrolyte ions (e.g., TDS) because these competitive metals have similar affinities for the same cell surface sites as the REEs. Using the known LFER relating metal-acetate and metal-bacteria stability constants shown (Figure S1), we found that the stability constant for cell surface complexation at 20 °C for La, a model REE, is similar in magnitude to that of U(VI), ~10−40% higher than for Pb and Cu, and >1300% higher than for Na. When ranked in order of decreasing metal competitiveness for bacterial surface sites, La(III) ≈ U(VI) > Pb(II) > Cu(II) ≫ Na(I). These results illustrate that the influence of Na and other weakly adsorbing metals, which constitute the majority of TDS, is clearly distinguishable from the effect of specifically competitive metals.

Effects of pH on REE Extraction Efficiency and Selectivity. The geofluids with higher total REE concentrations (e.g., > 100 ppb) are typically acidic (pH < 3.5), so a biosorbent that can function at lower pH is advantageous.[26] To test the effect of pH on REE biosorption, we conducted a series of Tb adsorption experiments with the GSL brine adjusted to an initial pH between 2 and 6. Higher pH conditions were not tested due to limited REE solubility.[9,16,27,51,52] Terbium was added in excess to avoid undersaturation of cell surface binding sites. We observed an increase in Tb extraction with increasing pH, peaking at ~5900 ± 1600 ppb at pH 6, and dropping to ~2000 ± 210 ppb at pH 2 (Figure 4a). As in the TDS experiments, the concentrations of major elements (Na, Mg, K, and Ca) in the eluent are generally <2% of those present in the initial GSL brine across the tested pH range (Figure 4b). At pH 6, there was a ~20-fold increase in REE purity in the eluent compared to the initial feedstock, which dropped to ~9-fold at pH 2 due to a decrease in the amount of Tb adsorbed.

To assess the effect of pH on REE recovery and selectivity more systematically, adsorption experiments were performed at varying cell densities (0 to ~2×10^9 cells/mL) and pH using a synthetic Horseshoe Spring (HS) geofluid (Table 1). The total REE concentration in the natural spring is 98 ppb and the solution has a pH of 3.5,[32] thus the synthetic solution was made with 100 ppb Nd and pH adjusted to 3−5 (Table S3). Neodymium, Na, Mg, K, and Ca solubility was minimally affected by pH within this range, while soluble Al and Fe concentrations decreased significantly (~64% and ~96%, respectively) as pH was adjusted from 3 to 5. Consistent with the GSL brine test, Nd adsorption efficiency was proportional to pH at a given cell density (Figure 5). Near complete REE recovery was observed at a cell density of ~4×10^8 cells/mL at pH 5 compared to only ~56% and ~38% recovery at pH 4 and 3, respectively. At a given pH, REE extraction efficiency increased with increasing cell density and ~100% extraction efficiency was reached for pH 3 and 4 at a cell concentration of 2×10^9 cells/mL (Figure 5; Table S3). These data suggest that increasing cell density can be an effective means to compensate for the reduction in adsorption efficiency at lower pH.

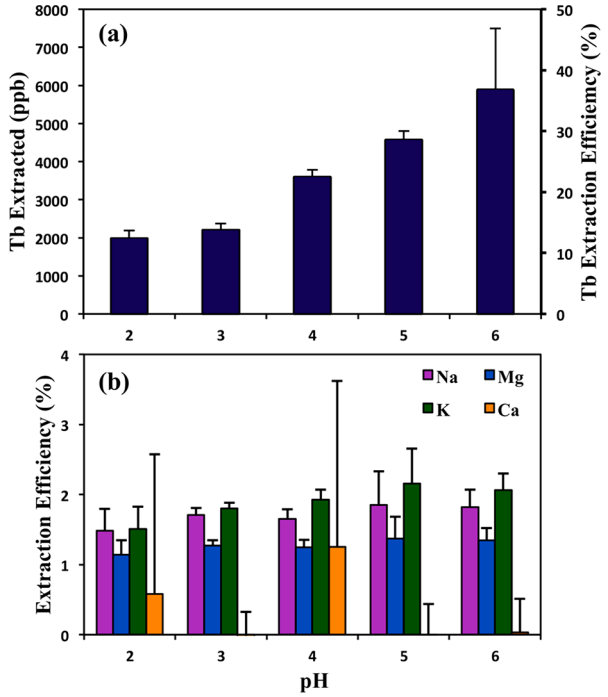

Figure 4. REE biosorption performance from the GSL brine at various pH conditions. Initial Tb concentration was fixed at ~16 ppm (100 μM) and cell concentration at ~1.2×10^9 cells/mL. (a) The amount of Tb recovered (ppb) and Tb extraction efficiency (%) increase with increasing pH (2−6). Less than 4% Tb loss was observed for abiotic controls at all tested pH conditions. (b) Extraction efficiency of major metals is <3% and shows no change over pH 2−6. The error bars represent the standard deviations of biological triplicates.

To determine how pH affects REE adsorption selectivity, non-REE adsorption was also quantified. Adsorption of Na, K, Mg, and Ca was not significant under all conditions, with the exception of Mg at pH 5, which further reinforces the efficacy of LBT-displayed cells to select against most non-REEs. Across all cell densities, the adsorbed REE purity generally increased with pH, largely due to the increase in REE adsorption. Al is the major non-REE contaminant at most pH and cell density conditions, and Al adsorption appears to be driven primarily by cell density rather than pH. The data highlight the effect of the biomass concentration on adsorbed REE purity. At pH 5, a high REE extraction efficiency can be achieved while retaining high purity; however, at lower pH, reaching a high REE extraction efficiency comes at a cost to REE purity. The highest adsorbed REE purity was observed at pH 5 with 2×10^8 cells/mL, while achieving a high Nd extraction efficiency of ~84% (Figure 5; Table S3). A further increase in cell density resulted in a reduction in purity due to increased Al adsorption. Notably, Mg adsorption only occurred at cell densities well beyond that required for 100% Nd extraction and after nearly complete adsorption of the more competitive Al (Figure 5). The highest Nd purity at pH 3 and 4 was achieved at cell densities of 2×10^8 and 9×10^8 cells/mL, respectively, which resulted in Nd extraction efficiencies of ~29% and ~68%, respectively. Collectively, these results demonstrate that recovery efficiency and selectivity can be manipulated by tailoring the adsorption conditions to the specific feedstock composition.

DOI: 10.1021/acs.est.9b00301
Environ. Sci. Technol. XXXX, XXX, XXX−XXX

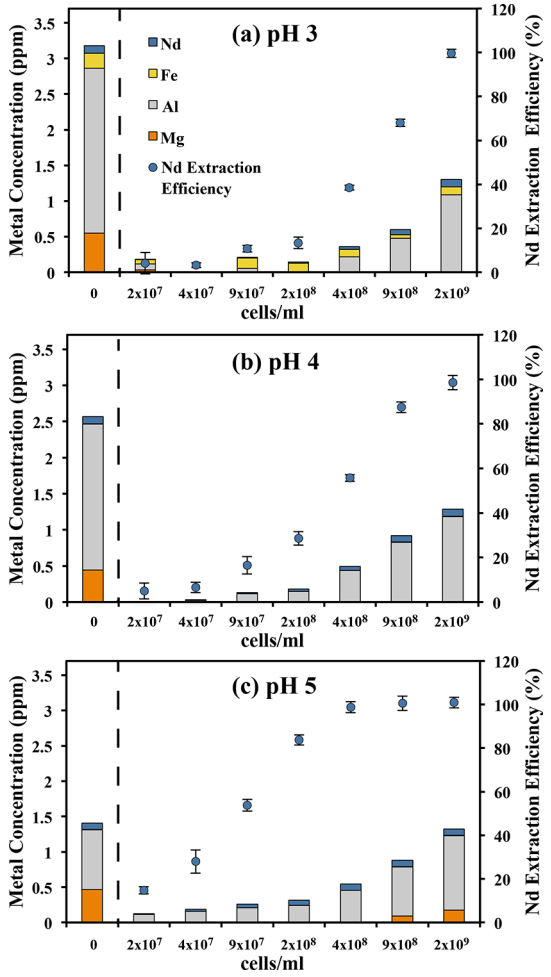

Figure 5. Nd extraction efficiency and purity as a function of pH and cell density. The Nd extraction efficiency (blue circles) and metal composition (stacked bars) of the adsorbed fraction was determined at varying cell densities for a synthetic Horseshoe Spring geofluid at (a) pH 3, (b) pH 4, and (c) pH 5. Measurements for Nd and three major non-REEs (Fe, Mg, and Al) are shown. Starting metal concentrations in the feedstock solution at varying pH were included as the bars on the far left. The error bars represent the standard deviations of biological duplicates.

Likely factors contributing to suppressed REE adsorption at lower pH include the protonation of cell surface binding sites and an increase in overall cell surface charge. The primary native cell surface functional groups involved in REE adsorption are carboxyl (pK_a, 4.3 and 5.5) and phosphoryl (pK_a, 2.2 and 6.9).[20−23] At low <4, phosphoryl ligands are expected to exert a dominant control on REE adsorption, and carboxyl ligands play a larger role as pH increases,[53] which is reflected in the REE adsorption data in which adsorption decreases with pH, especially below pH 4. Consistent with previous studies,[51,52,54−56] we conclude that the optimal REE adsorption by the LBT-displayed strain of *E. coli* occurs at pH 5−6.

Effects of Temperature. Since geothermal fluids range from ambient temperatures to >300 °C, we examined REE adsorption efficiency as a function of temperature. A series of adsorption experiments with the synthetic GSL brine were conducted at 24, 40, and 70 °C. A high Tb concentration (~48 ppm) was set to exceed the apparent adsorption capacity of the cells at room temperature. Although cells are no longer viable at 70 °C, they appear to remain structurally intact as examined via light microscopy (Figure S2). While there was minimal change in Tb adsorption from 24 to 40 °C in the high TDS GSL brine, REE adsorption nearly tripled (~2.9-fold) from 40 to 70 °C (Figure 6a). Further temperature increase to 100 °C did not yield additional improvement in extraction efficiency (Figure S3). The increase in purity improved from ~15-fold at 24 °C to ~60-fold at 70 °C. Less than 1% of the major elements were recovered at all tested temperatures (Figure 6b). The increase in the extraction efficiency of REEs but not major elements suggests that a biosorption operation at elevated temperatures (e.g., 70 °C) may improve REE extraction efficiency without compromising REE purity. We performed a series of experiments and constructed a theoretical model to better understand this intriguing REE biosorption behavior at elevated temperatures.

To determine if the temperature dependence of Tb adsorption was impacted by the high TDS in the GSL brine or was an innate feature of the cell surface, we conducted monoelement biosorption experiments in the low TDS buffer solution (10 mM MES pH 6) at 24, 40, and 70 °C. Terbium adsorption in MES buffer exhibited an approximately linear increase in extraction efficiency with increasing temperature, with a smaller increase (~1.6-fold) compared to the GSL brine (~2.9-fold) from 24 to 70 °C (Figure 6c). Prior studies have similarly revealed that temperature dependence of Mg and Ca adsorption onto mineral surfaces was variably affected by ionic strength.[57,58] Major element (Mg, K, Ca) adsorption in the buffer solution exhibited no systematic change with temperature (Figure 6c); Na was not tested due to the non-negligible Na present in MES. The increased Tb adsorption efficiency and selectivity with increasing temperature is therefore not likely controlled by aqueous speciation in the GSL feedstock, but rather is characteristic of the cell surface.

To examine whether the temperature dependence of REE adsorption is caused by a temporary, reversible change in adsorption behavior or a permanent change in cell envelope structure, we analyzed the REE extraction efficiency of cells that were heated to 70 °C then cooled to 24 °C prior to REE exposure. These cells exhibited the same extraction efficiency as unheated cells, indicating that the increased Tb adsorption at elevated temperatures is reversible (Figure 6d). Moreover, UV-killed cells exhibited the same Tb extraction efficiency as live cells, suggesting that cell vitality has no effect on REE adsorption (Figure 6d). A change in adsorption kinetics is also unlikely to explain the temperature dependence since maximum adsorption occurs within 5 min at room temperature (Table S3), and the incubation time of 25 min ensured that equilibrium was reached for all experiments. Together, these observations provide strong evidence that the observed increase in REE extraction efficiency and selectivity with increasing temperature likely results from innate thermodynamic properties of the cell surface functional groups.

Thermodynamic Analysis of Temperature-Dependent Biosorption. Changes in temperature have been shown to directly impact the thermodynamics of metal complexation by surface ligands. For example, complexation of many metals by carboxylate complexes on biological surfaces tends to be endothermic, resulting in enhanced metal adsorption at higher temperatures.[59] This behavior has been attributed to a reversible increase in the enthalpy of REE inner sphere complexation with cell surface functional groups.[28−30]

DOI: 10.1021/acs.est.9b00301
Environ. Sci. Technol. XXXX, XXX, XXX−XXX

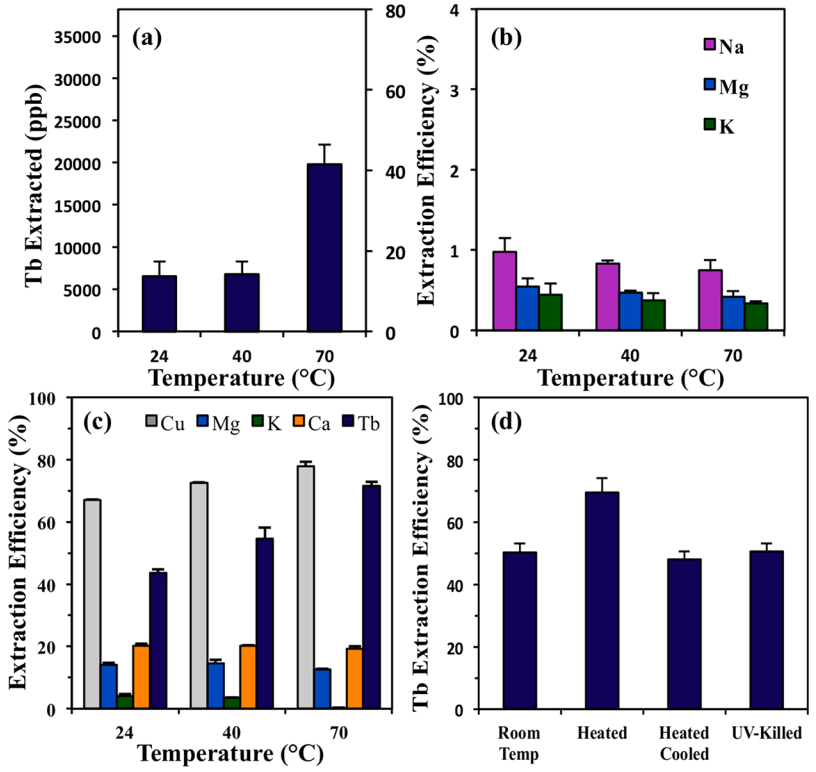

Figure 6. (a) REEs extracted (ppb) and extraction efficiency (%) from the GSL brine as a function of temperature from 24 to 70 °C. The initial Tb concentration was ~48 ppm and the cell concentration was ~1.2×10^9 cells/mL. Less than 3% Tb extraction was observed for abiotic controls at all temperatures. (b) Extraction efficiency (%) from the GSL brine remains <2% for the major metals at all tested temperatures. (c) Tb, Cu, Mg, K, and Ca extraction efficiencies as a function of temperature from 24 to 70 °C in 10 mM MES pH 6. (d) Comparison of Tb extraction efficiency in buffer solution at room temperature (24 °C), heated (70 °C), heated to 70 °C then cooled to 24 °C before Tb exposure, and UV-killed cells at 24 °C. The error bars represent the standard deviations of biological triplicates.

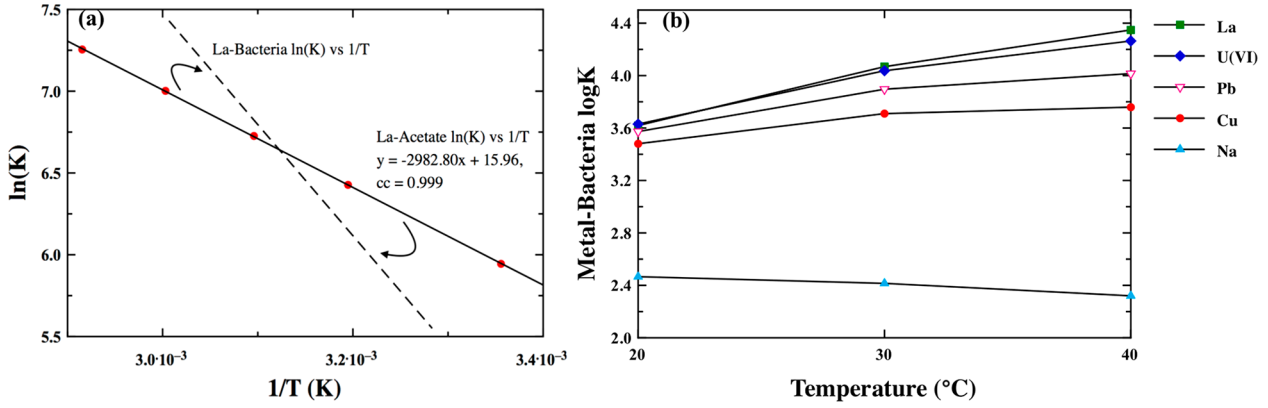

Figure 7. (a) Van't Hoff plots of lanthanum-acetate and projected lanthanum-bacteria complexation. The lanthanum-bacteria ln(K) vs $1/T$ plot is a qualitative dashed line indicating a steeper negative slope than lanthanum-acetate given that the lanthanum-bacteria stability constant is higher than its lanthanum-acetate counterpart at elevated temperatures. (b) Metal-bacteria stability constants (log K) as a function of temperature. Stability constants for La, U(VI), Cu, and Na (closed symbols) were calculated based on a temperature-dependent linear free energy relationship (Figure S1) generated from Zn, Cd, and Pb-acetate[34] and bacteria (open symbol) stability constant data.[35]

Fein et al. (2001) constructed a linear free energy relationship (LFER) at ambient temperature to relate metal-acetate and metal-*Bacillus subtilis* complexation stability constants, reporting a high 0.97 linear correlation coefficient for numerous metals including neodymium (Nd). The stability of aqueous REE-acetate complexes is known to increase with temperature,[34] but the corresponding REE-bacteria stability constants are unknown at elevated temperatures. We developed a series of temperature-dependent LFERs based on available metal-bacteria stability constants for *Penicillium simplicissimum* biosorption of Zn(II), Cd(II), and Pb(II) at 24, 30, and 40 °C. The slopes of these LFERs steepen with increasing temperature, indicating that metal-bacteria stability constants increase more quickly with temperature than the corresponding metal-acetate stability constants (Figure S1).[35] A Van't Hoff plot for aqueous REE-acetate complexation stability constants was constructed using thermodynamic data from Ding and Wood (2002) (Figure 7a).[36] The slope of the

DOI: 10.1021/acs.est.9b00301
Environ. Sci. Technol. XXXX, XXX, XXX−XXX

Van't Hoff plot gives a positive $\Delta H_{La\text{-}Acetate}$ of 24.8 kJ/mol, indicating an endothermic reaction. On the basis of the temperature dependence of calculated LFERs, the slope of the REE-bacteria Van't Hoff plot is expected to be steeper (i.e., more negative) than its corresponding REE-acetate plot (Figure 7a), which strongly suggests that REE-bacterial surface complexation reactions are even more endothermic. We conclude that the strong positive temperature dependence of REE biosorption is likely controlled by the increased REE affinity for carboxylate functional groups on the cell surface.

The same LFER analysis can be used to evaluate the influence of temperature on bacterial surface selectivity for various metals. At higher temperatures, La-bacteria stability constants increase more dramatically than those of the competitive metals included for comparison (Na, Zn, Cd, Cu, and Pb, Figure 7b). Thus, increasing temperature is expected to cause both increased REE adsorption and increased surface selectivity for the REEs. The apparent increase in surface selectivity for REEs with respect to the competitive metals in the GSL brine can be explained by the proportionally greater increase in REE-surface site affinity compared with non-REEs with increasing temperature, as indicated in Figure 7b. On the basis of the good agreement between the experimental data and the theoretical thermodynamic behavior, we conclude that the observed increase in Tb adsorption with increasing temperature is likely a thermodynamic effect, although reversible, temperature-mediated changes to the cell surface cannot be conclusively ruled out.

Implications for REE Extraction. Given its high REE recovery efficiency and selectivity, biosorption with LBT-displayed *E. coli* shows promise for REE recovery from geofluids. In an integrated biosorption-based REE recovery process, the first step is to precondition the geofluid to optimal conditions for biosorption (e.g., pH 5−6 and 70 °C) to maximize adsorption while retaining REE solubility. As a result of the temperature and pH changes, the solubility of some competitive metals, particularly Al and Fe, will be limited. Therefore, the removal of precipitates prior to biosorption is expected to alleviate competitive adsorption by these contaminants. Following preconditioning, selective biosorption will deliver a REE-enriched eluent, from which REEs can be precipitated as mineral phases by adding oxalate or carbonate. Unlike REEs, some metals, such as U, will remain in solution during precipitation, improving REE purity.[17,49] Finally, the REE precipitates can be roasted to produce total rare earth oxides. Overall, this study contributes to the development of innovative clean mining technologies through the demonstration of selective biosorption using bioengineered microbes as an effective platform for extracting REEs from geofluids.

■ ASSOCIATED CONTENT

Supporting Information

The Supporting Information is available free of charge on the ACS Publications website at DOI: 10.1021/acs.est.9b00301.

Tables S1, metal concentration profile of the BMG before and after biosorption; Table S2, metal recovery from the GSL brine at different TDS; Table S3, metal recovery from the HS geothermal fluid at a range of cell densities and pH conditions; Table S4, Tb biosorption kinetics; Figure S1, modeled linear free energy relationship dependence on temperature for metal−cell surface and metal−acetate complexation; Figure S2, live/dead staining of heated and cooled cells; and Figure S3, temperature dependence of REE recovery up to 100 °C (PDF)

■ AUTHOR INFORMATION

Corresponding Author

*E-mail: jiao1@llnl.gov.

ORCID

Yat Li: 0000-0002-8058-2084

Yongqin Jiao: 0000-0002-6798-5823

Notes

The authors declare no competing financial interest.

■ ACKNOWLEDGMENTS

We thank Geoffrey Garrison at AltaRock for providing the Blue Mountain geothermal fluid and Hari Neupane at Idaho National Laboratory for providing the Great Salt Lake brine. This research is supported by the U.S. Department of Energy, Office of Energy Efficiency and Renewable Energy, Geothermal Office. AB acknowledges funding from the Livermore Graduate Scholar Program from Lawrence Livermore National Laboratory. This work was performed under the auspices of the U.S. Department of Energy by Lawrence Livermore National Laboratory under Contract DEAC52-07NA27344 (LLNL-JRNL-751666).

■ REFERENCES

(1) DOE. Critical Materials Strategy. In 2011.

(2) Eggert, R.; Wadia, C.; Anderson, C.; Bauer, D.; Fields, F.; Meinert, L.; Taylor, P. Rare Earths: Market Disruption, Innovation, and Global Supply Chains. *Annual Review of Environment and Resources* **2016**, *41* (1), 199−222.

(3) Zhou, B.; Li, Z.; Chen, C. Global potential of rare earth resources and rare earth demand from clean technologies. *Minerals* **2017**, *7*, 203.

(4) Zhuang, W. Q.; Fitts, J. P.; Ajo-Franklin, C. M.; Maes, S.; Alvarez-Cohen, L.; Hennebel, T. Recovery of critical metals using biometallurgy. *Curr. Opin. Biotechnol.* **2015**, *33*, 327−335.

(5) Hennebel, T.; Boon, N.; Maes, S.; Lenz, M. Biotechnologies for critical raw material recovery from primary and secondary sources: R&D priorities and future perspectives. *New Biotechnol.* **2015**, *32* (1), 121−127.

(6) Dodson, J. R.; Parker, H. L.; Garcia, A. M.; Hicken, A.; Asemave, K.; Farmer, T. J.; He, H.; Clark, J. H.; Hunt, A. J. Bio-derived materials as a green route for precious & critical metal recovery and re-use. *Green Chem.* **2015**, *17* (4), 1951−1965.

(7) Eggert, R.; Wadia, C.; Anderson, C.; Bauer, D.; Fields, F.; Meinert, L.; Taylor, P. Rare Earths: Market disruption, innovation, and global supply chains. *Annu. Rev. Environ. Resour.* **2016**, *41*, 199−222.

(8) Jacinto, J.; Henriques, B.; Duarte, A. C.; Vale, C.; Pereira, E. Removal and recovery of Critical Rare Elements from contaminated waters by living Gracilaria gracilis. *J. Hazard. Mater.* **2018**, *344*, 531−538.

(9) Kucuker, M. A.; Wieczorek, N.; Kuchta, K.; Copty, N. K. Biosorption of neodymium on Chlorella vulgaris in aqueous solution obtained from hard disk drive magnets. *PLoS One* **2017**, *12* (4), No. e0175255.

(10) Lo, Y. C.; Cheng, C. L.; Han, Y. L.; Chen, B. Y.; Chang, J. S. Recovery of high-value metals from geothermal sites by biosorption and bioaccumulation. *Bioresour. Technol.* **2014**, *160*, 182−190.

(11) Jiang, M. Y.; Ohnuki, T.; Tanaka, K.; Kozai, N.; Kamiishi, E.; Utsunomiya, S. Post-adsorption process of Yb phosphate nanoparticle formation by Saccharomyces cerevisiae. *Geochim. Cosmochim. Acta* **2012**, *93*, 30−46.

DOI: 10.1021/acs.est.9b00301
Environ. Sci. Technol. XXXX, XXX, XXX−XXX

(12) Moriwaki, H.; Yamamoto, H. Interactions of microorganisms with rare earth ions and their utilization for separation and environmental technology. *Appl. Microbiol. Biotechnol.* **2013**, *97* (1), 1−8.
(13) Ozaki, T.; Gillow, J. B.; Kimura, T.; Ohnuki, T.; Yoshida, Z.; Francis, A. J. Sorption behavior of europium(III) and curium(III) on the cell surfaces of microorganisms. *Radiochim. Acta* **2004**, *92* (9−11), 741−748.
(14) Texier, A. C.; Andres, Y.; Le Cloirec, P. Selective biosorption of lanthanide (La, Eu, Yb) ions by Pseudomonas aeruginosa. *Environ. Sci. Technol.* **1999**, *33* (3), 489−495.
(15) Tsuruta, T. Accumulation of rare earth elements in various microorganisms. *J. Rare Earths* **2007**, *25* (5), 526−532.
(16) Park, D. M.; Reed, D. W.; Yung, M. C.; Eslamimanesh, A.; Lencka, M. M.; Anderko, A.; Fujita, Y.; Riman, R. E.; Navrotsky, A.; Jiao, Y. Q. Bioadsorption of Rare Earth Elements through Cell Surface Display of Lanthanide Binding Tags. *Environ. Sci. Technol.* **2016**, *50* (5), 2735−2742.
(17) Nash, K. L.; Jensen, M. P. Analytical-scale separations of the lanthanides: A review of techniques and fundamentals. *Sep. Sci. Technol.* **2001**, *36* (5−6), 1257−1282.
(18) Xie, F.; Zhang, T. A.; Dreisinger, D.; Doyle, F. A critical review on solvent extraction of rare earths from aqueous solutions. *Miner. Eng.* **2014**, *56*, 10−28.
(19) Park, D. M.; Brewer, A.; Reed, D. W.; Lammers, L. N.; Jiao, Y. Recovery of Rare Earth Elements from Low-Grade Feedstock Leachates Using Engineered Bacteria. *Environ. Sci. Technol.* **2017**, *51* (22), 13471−13480.
(20) Ngwenya, B. T.; Magennis, M.; Olive, V.; Mosselmans, J. F.; Ellam, R. M. Discrete site surface complexation constants for lanthanide adsorption to bacteria as determined by experiments and linear free energy relationships. *Environ. Sci. Technol.* **2010**, *44* (2), 650−6.
(21) Martinez, R. E.; Pourret, O.; Takahashi, Y. Modeling rare earth element sorption to the Gram positive Bacillus subtilis bacteria surface. *J. Colloid Interface Sci.* **2014**, *413*, 106−111.
(22) Markai, S.; Andres, Y.; Montavon, G.; Grambow, B. Study of the interaction between europium (III) and Bacillus subtilis: fixation sites, biosorption modeling and reversibility. *J. Colloid Interface Sci.* **2003**, *262*, 351−361.
(23) Texier, A. C.; Andres, Y.; Illemassene, M.; Le Cloirec, P. Characterization of lanthanide ions binding sites in the cell wall of Pseudomonas aeruginosa. *Environ. Sci. Technol.* **2000**, *34* (4), 610−615.
(24) Smith, Y. R.; Kumar, P.; McLennan, J. D. On the Extraction of Rare Earth Elements from Geothermal Brines. *Resources-Basel* **2017**, *6* (3), 39.
(25) Jin, H. Y.; Park, D. M.; Gupta, M.; Brewer, A. W.; Ho, L.; Singer, S. L.; Bourcier, W. L.; Woods, S.; Reed, D. W.; Lammers, L. N.; Sutherland, J. W.; Jiao, Y. Q. Techno-economic Assessment for Integrating Biosorption into Rare Earth Recovery Process. *ACS Sustainable Chem. Eng.* **2017**, *5* (11), 10148−10155.
(26) Wood, S. A. Behavior of rare earth elements in geothermal systems: A new exploration/exploitation tool? In DOE, Ed. *Geothermal Reservoir Technology Research*; 2001.
(27) Bonificio, W. D.; Clarke, D. R. Rare-Earth Separation Using Bacteria. *Environ. Sci. Technol. Lett.* **2016**, *3* (4), 180−184.
(28) Takahashi, Y.; Chatellier, X.; Hattori, K. H.; Kato, K.; Fortin, D. Adsorption of rare earth elements onto bacterial cell walls and its implication for REE sorption onto natural microbial mats. *Chem. Geol.* **2005**, *219* (1−4), 53−67.
(29) Smith, Y. R.; Bhattacharyya, D.; Willhard, T.; Misra, M. Adsorption of aqueous rare earth elements using carbon black derived from recycled tires. *Chem. Eng. J.* **2016**, *296*, 102−111.
(30) Xu, S. X.; Wang, Z. W.; Gao, Y. Q.; Zhang, S. M.; Wu, K. Adsorption of Rare Earths(III) Using an Efficient Sodium Alginate Hydrogel Cross-Linked with Poly-gamma-Glutamate. *PLoS One* **2015**, *10* (5), e0124826.
(31) Muravyov, M. I.; Bulaev, A. G.; Melamud, V. S.; Kondrat'eva, T. F. [Leaching of Rare Earth Elements from Coal Ashes Using Acidophilic Chemolithotrophic Microbial Communities]. *Microbiology* **2015**, *84* (2), 194.
(32) Lewis, A. J.; Palmer, M. R.; Sturchio, N. C.; Kemp, A. J. The rare earth element geochemistry of acid-sulphate and acid-sulphate-chloride geothermal systems from Yellowstone National Park, Wyoming, USA. *Geochim. Cosmochim. Acta* **1997**, *61* (4), 695−706.
(33) Fein, J. B.; Martin, A. M.; Wightman, P. G. Metal adsorption onto bacterial surfaces: Development of a predictive approach. *Geochim. Cosmochim. Acta* **2001**, *65* (23), 4267−4273.
(34) Shock, E. L.; Koretsky, C. M. Metal-organic complexes in geochemical processes: Calculation of standard partial molal thermodynamic properties of aqueous acetate complexes at high pressures and temepratures. *Geochim. Cosmochim. Acta* **1993**, *57* (20), 4899−4922.
(35) Fan, T.; Liu, Y.; Feng, B.; Zeng, G.; Yang, C.; Zhou, M.; Zhou, H.; Tan, Z.; Wang, X. Biosorption of cadmium(II), zinc(II) and lead(II) by Penicillium simplicissimum: Isotherms, kinetics and thermodynamics. *J. Hazard. Mater.* **2008**, *160* (2−3), 655−61.
(36) Ding, R. W. S. A. The aqueous geochemistry of the rare earth elements and yttrium. Part X. Potentiometric determination of stability constants of acetate complexes of La^{3+}, Nd^{3+}, Gd^{3+}, and Yb^{3+} at 25−70 °C and 1 bar. In *Water-Rock Interactions, Ore Deposits, And Environmental Geochemistry: A Tribute to David A.*; Crerar, R., Hellmann, S. A. W., Eds.; The Geochemical Society: 2002; pp 209−227.
(37) Fournier, P.; Oelkers, E. H.; Gout, R.; Pokrovski, G. Experimental determination of aqueous sodium-acetate dissociation constants at temperatures from 20 to 240 degrees C. *Chem. Geol.* **1998**, *151* (1−4), 69−84.
(38) Jiang, J.; Rao, L.; Di Bernardo, P.; Zanonato, P. L.; Bismondo, A. Complexation of uranium(VI) with acetate at variable temperatures. *J. Chem. Soc., Dalton Trans.* **2002**, No. 8, 1832−1838.
(39) Martin, L. J.; Hahnke, M. J.; Nitz, M.; Wohnert, J.; Silvaggi, N. R.; Allen, K. N.; Schwalbe, H.; Imperiali, B. Double-lanthanide-binding tags: Design, photophysical properties, and NMR applications. *J. Am. Chem. Soc.* **2007**, *129* (22), 7106−7113.
(40) Ngwenya, B. T.; Mosselmans, J. F. W.; Magennis, M.; Atkinson, K. D.; Tourney, J.; Olive, V.; Ellam, R. M. Macroscopic and spectroscopic analysis of lanthanide adsorption to bacterial cells. *Geochim. Cosmochim. Acta* **2009**, *73* (11), 3134−3147.
(41) Munemoto, T.; Ohmori, K.; Iwatsuki, T. Rare earth elements (REE) in deep groundwater from granite and fracture-filling calcite in the Tono area, central Japan: Prediction of REE fractionation in paleo- to present-day groundwater. *Chem. Geol.* **2015**, *417*, 58−67.
(42) Tang, J. W.; Johannesson, K. H. Rare earth elements adsorption onto Carrizo sand: Influence of strong solution complexation. *Chem. Geol.* **2010**, *279* (3−4), 120−133.
(43) Small, T. D.; Warren, L. A.; Ferris, F. G. Influence of ionic strength on strontium sorption to bacteria, Fe(III) oxide, and composite bacteria-Fe(III) oxide surfaces. *Appl. Geochem.* **2001**, *16* (7−8), 939−946.
(44) Borrok, D. M.; Fein, J. B. The impact of ionic strength on the adsorption of protons, Pb, Cd, and Sr onto the surfaces of Gram negative bacteria: testing non-electro static, diffuse, and triple-layer models. *J. Colloid Interface Sci.* **2005**, *286* (1), 110−126.
(45) Daughney, C. J.; Fein, J. B. The effect of ionic strength on the adsorption of H+, Cd2+, Pb2+, and Cu2+ by Bacillus subtilis and Bacillus licheniformis: A surface complexation model. *J. Colloid Interface Sci.* **1998**, *198* (1), 53−77.
(46) Elsalamouny, A. R.; Desouky, O. A.; Mohamed, S. A.; Galhoum, A. A.; Guibal, E. Uranium and neodymium biosorption using novel chelating polysaccharide. *Int. J. Biol. Macromol.* **2017**, *104*, 963−968.
(47) Poetsch, M.; Lippold, H. Effects of ionic strength and fulvic acid on adsorption of Tb(III) and Eu(III) onto clay. *J. Contam. Hydrol.* **2016**, *192*, 146−151.

DOI: 10.1021/acs.est.9b00301
Environ. Sci. Technol. XXXX, XXX, XXX−XXX

(48) Dolatyari, L. Y.; Yaftian, R. M.; Rostamnia, S. Adsorption characteristics of Eu(III) and Th(IV) ions onto modified mesoporous silica SBA-15 materials. *J. Taiwan Inst. Chem. Eng.* **2016**, *60*, 174−184.
(49) Zhu, Z.; Pranolo, Y.; Cheng, C. Y. Separation of uranium and thorium from rare earths for rare earth production - A review. *Miner. Eng.* **2015**, *77*, 185−196.
(50) Mashkovtsev, M. B. M.; Smyshlyaev, D.; Pajarre, R.; Kangas, P.; Rychkov, V.; Koukkari, P. Pilot-scale recovery of rare earths and scandium from phosphogypsum and uranium leachates. *E3S Web of Conferences* 2016, *8* (01026).
(51) Hosomomi, Y.; Wakabayashi, R.; Kubota, F.; Kamiya, N.; Goto, M. Diglycolic amic acid-modified E. coli as a biosorbent for the recovery of rare earth elements. *Biochem. Eng. J.* **2016**, *113*, 102−106.
(52) Vijayaraghavan, K.; Sathishkumar, M.; Balasubramanian, R. Interaction of rare earth elements with a brown marine alga in multi-component solutions. *Desalination* **2011**, *265* (1−3), 54−59.
(53) Takahashi, Y.; Yamamoto, M.; Yamamoto, Y.; Tanaka, K. EXAFS study on the cause of enrichment of heavy REEs on bacterial surfaces. *Geochim. Cosmochim. Acta* **2010**, *74*, 5443−5462.
(54) Mosbah, R.; Sahmoune, M. N. Biosorption of heavy metals by Streptomyces species - an overview. *Cent Eur. J. Chem.* **2013**, *11* (9), 1412−1422.
(55) Pacheco, P. H.; Gil, R. A.; Cerutti, S. E.; Smichowski, P.; Martinez, L. D. Biosorption: A new rise for elemental solid phase extraction methods. *Talanta* **2011**, *85* (5), 2290−2300.
(56) Xu, S. X.; Zhang, S. M.; Chen, K.; Han, J. F.; Liu, H. S.; Wu, K. Biosorption of La3+ and Ce3+ by Agrobacterium sp HN1. *J. Rare Earths* **2011**, *29* (3), 265−270.
(57) Ridley, M. K.; Machesky, M. L.; Wesolowski, D. J.; Palmer, D. A. Calcium adsorption at the rutile-water interface: A potentiometric study in NaCl media to 250C. *Geochim. Cosmochim. Acta* **1999**, *63*, 3087−3096.
(58) Katz, L. E.; Criscenti, L. J.; Chen, C. C.; Larentzos, J. P.; Liljestrand, H. M. Temperature effects on alkaline earth metal ions adsorption on gibbsite: approaches from macroscopic sorption experiments and molecular dynamics simulations. *J. Colloid Interface Sci.* **2013**, *399*, 68−76.
(59) Sag, Y.; Kutsal, T. Determination of the biosorption heats of heavy metal ions on *Zoogloea ramigera* and *Rhizopus arrhizus*. *Biochem. Eng. J.* **2000**, *6*, 145−151.
(60) Shakeri, A.; Ghoreyshinia, S.; Mehrabi, B.; Delavari, M. Rare earth elements geochemistry in springs from Taftan geothermal area SE Iran. *J. Volcanol. Geotherm. Res.* **2015**, *304*, 49−61.
(61) Sanada, T.; Takamatsu, N.; Yoshiike, Y. Geochemical interpretation of long-term variations in rare earth element concentrations in acidic hot spring waters from the Tamagawa geothermal area, Japan. *Geothermics* **2006**, *35* (2), 141−155.
(62) Zhang, Y.; Tan, H.; Zhang, W.; Wei, H.; Dong, T. Geochemical constraint on origin and evolution of solutes in geothermal springs in western Yunnan, China. *Chem. Erde* **2016**, *76*, 63−75.
(63) Michard, A. Rare earth element systematics in hydrothermal fluids. *Geochim. Cosmochim. Acta* **1989**, *53*, 745−750.

DOI: 10.1021/acs.est.9b00301
Environ. Sci. Technol. XXXX, XXX, XXX−XXX